Available online at www.sciencedirect.com
SCIENCE DIRECT
Polymer 46 (2005) 1878–1885
polymer
www.elsevier.com/locate/polymer

Crystallization of polyethylene under shear flow as studied by time resolved depolarized light scattering. Effects of shear rate and shear strain

H. Fukushima, Y. Ogino, G. Matsuba, K. Nishida, T. Kanaya*

Institute for Chemical Research, Kyoto University, Uji, Kyoto-fu 611-0011, Japan

Received 8 September 2004; received in revised form 22 December 2004; accepted 28 December 2004
Available online 21 January 2005

Abstract

We have studied structure formation during crystallization of polyethylene (PE) under shear flow using time resolved depolarized light scattering (DPLS) in order to elucidate the formation mechanism of the so-called shish-kebab structure. Two-dimensional (2D) DPLS pattern clearly showed streak-like scattering normal to the flow direction in the early stage during the crystallization after pulse shear, suggesting the formation of the shish-like structure in μm scale. In order to analyze the 2D DPLS pattern we defined measures for the acceleration of the crystallization rate and the degree of anisotropy and found that there are critical shear rates for both of the acceleration and the anisotropy at a given shear strain: the former is much smaller than the latter. We also determined the critical shear rate for the anisotropy as a function of the shear strain. Extrapolating to inverse of the infinite shear strain = 0, we found the critical shear rate for the anisotropy at the infinite shear strain to be 1.5 s^{-1}. The results were discussed in relation to a competition between the relaxation rate of polymer chains and the orientation-induced crystallization rate.

Keywords: Crystallization; Shear flow; Shish-kebab

1. Introduction

Extensive studies have been carried out on polymer crystallization under flow like elongational and shear flows from both industrial and scientific points of view [1–4]. In many polymer processing operations such as fiber spinning, injection molding and extrusion, polymers experience various kinds of flows and the crystallization kinetics and the final morphology are greatly affected by the flows. It is known [5–9] that when polymers in melts and solutions are crystallized under elongational and/or shear flows the so-called shish-kebab structure is often formed, which consist of long central fiber core (shish) surrounded by lamellar crystalline structure (kebab) periodically attached along the shish. It is believed that the shish is formed by crystallization of completely stretched polymer chains and the kebabs are folded chain lamella crystals and grow to the direction normal to the shish. Recent development of advanced characterization techniques such as in situ rheo-small-angel and wide-angle X-ray scattering (SAXS and WAXS) [10–20] and in situ rheo-small-angle light scattering (SALS) [21–23] and rheo-optical measurements [24–26] has shed light on significant features of the formation mechanism of the shish-kebab structure. In situ rheo-SAXS and rheo-WAXS measuremetns were extensively carried out on the structure development in fiber spinning process [10,11,13–15,27,28] as well as in shear-induced crystallization process [12,16–18,20]. Some of the works have focused on the structural formation in the early stage of the crystallization under flow using "short term shearing" technique [29] because it often governs or at least affect the final structure deeply. In situ rheo-SAXS and rheo-WAXS studies on iPP and polyethylene (PE) after pulse shear by Hsiao et al. [18,20] have shown that a scaffold or network of oriented structures is formed prior to the full-crystallization. Kornfield et al. [24–26] have preformed in situ birefringence measurements on isotactic polypropylene (iPP) after short term shearing, and found that the

* Corresponding author. Tel.: +81 774 38 3140; fax: +81 774 38 3146.
E-mail address: kanaya@scl.kyoto-u.ac.jp (T. Kanaya).

0032-3861/$ - see front matter © 2005 Elsevier Ltd. All rights reserved.
doi:10.1016/j.polymer.2004.12.048

birefringence drops after the shear but shows upturn again, suggesting formation of a precursor of the shish-kebab structure. These studies have indicated that a precursor of the shish is formed in the very early stage during the crystallization process after the shear. A pioneering in situ rheo-SALS study by Katayama et al. [30] also demonstrated that there exists a mesomorphic state during the shear-induced crystallization process about 30 years ago. Recent in situ rheo SALS measurements on iPP by Winter et al. [21–23] have revealed that density fluctuations occurs before the orientation fluctuations. Despite the extensive studies, the formation mechanism of the shish-kebab structure is not fully understood. One of the reasons is that there are many factors which influence the formation of the shish-kebab structure such as molecular weight, molecular weight distribution, branching in chain, shear rate, shear strain, crystallization temperature and so on. It is necessary in such situation to perform systematic studies on the crystallization process as a function of each factor to elucidate the formation mechanism.

In this study, focusing on the effects of shear rate as well as shear strain, we investigated the structural formation of PE in the early stage of crystallization under shear flow using time resolved depolarized light scattering (DPLS) technique. For this purpose we have also employed short term shearing technique or pulse shear technique [29]. The PE used in the study has rather low molecular weight and rather wide molecular weight distribution as will be mentioned in the experimental part. The low molecular weight allows us to perform the experiment in wide ranges of shear rate and sear strain. In addition, we empirically know that the shish-kebab formation is enhanced in samples with wide molecular weight distribution compared with the narrow one. This may suggest an important role of the high molecular weight component in the shish-kebab formation. This problem will be discussed in a forthcoming paper.

2. Experimental

Here we used polyethylene with molecular weight $M_w =$ 58,600 and the polydispersity $M_w/M_n = 8.01$, where M_w and M_n are the weight- and number-average molecular weight, respectively. The PE was kindly supplied by Showa Denko Ltd. The nominal melting temperature of the PE determined by DSC measurements was 134 °C at the heating rate of 20 °C/min.

DSC measurements were carried out to characterize the thermal properties of the sample using Perkin–Elmer DSC-7. All the DSC scans were performed under nitrogen environment.

Two-dimensional (2D) depolarized light scattering (DPLS) measurements were carried out using a home-made apparatus with He–Ne laser (80 mW, wavelength $\lambda =$ 633 nm) as a light source and 2D screen and CCD camera as a detector system. The range of length of scattering vector Q in this experiment is 4×10^{-5} to 2.6×10^{-4} Å^{-1}, where Q is given by $Q = 4\pi\sin\theta/n\lambda$ (2θ and n being scattering angle and the refractive index, respectively).

A Linkam CSS-450 high temperature shear cell with quartz windows was used to control the temperature and the shear conditions. The sample thickness in the cell was 300 μm for all the DPLS measurements. The temperature protocol for the shear experiments is shown in Fig. 1: (a) the polymer sample was heated up to 165 °C from room temperature at a rate of 30 °C/min, (b) held at 165 °C for 5 min, (c) cooled down to the crystallization temperature $T_c = 129$ °C at a rate of 30 °C/min, and then (d) held at 129 °C for the DPLS measurements. The polymer melt was subjected to pulse shear just after reaching the crystallization temperature T_c of 129 °C. The ranges of the shear rate and the shear strain were 0–32 s^{-1} and 800–19,200%, respectively.

3. Results and discussion

Fig. 2 shows the time evolutions of the 2D DPLS patterns under quiescent crystallization condition ($\dot\gamma = 0$ s^{-1}) and after pulse shear with shear rate $\dot\gamma = 16$ s^{-1} and shear strain $\varepsilon = 3200\%$. Under the quiescent condition, no scattering intensity is observed in the first 110 s after reaching T_c, corresponding to the so-called induction period, and then isotropic 2D DPLS pattern appears and increases in intensity with annealing time as seen in the upper row in Fig. 2. On the other hand, under the shear condition with $\dot\gamma = 16$ s^{-1} and $\varepsilon = 3200\%$, very weak anisotropic scattering pattern begins to appear at about 30 s after applying the pulse shear. This indicates that there are long scattering objects aligned along the flow direction, which must be the shish-like structure. The length of shish-like structure is in μm order judging from the scattering vector range in the DPLS measurements. Exact size evaluation of the shish-like structure will be reported in a separated paper. It is no doubt that the shish-like structure is formed by the effect of the pulse shear because the 2D pattern under the quiescent condition does not show any anisotropic scattering. The anisotropic streak-like scattering pattern gradually increases

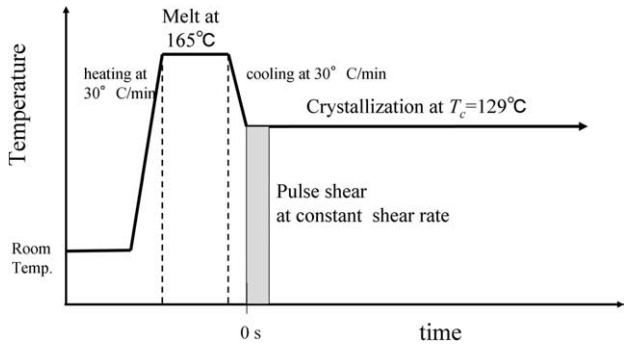

Fig. 1. Temperature protocol for the shear experiments on polyethylene.

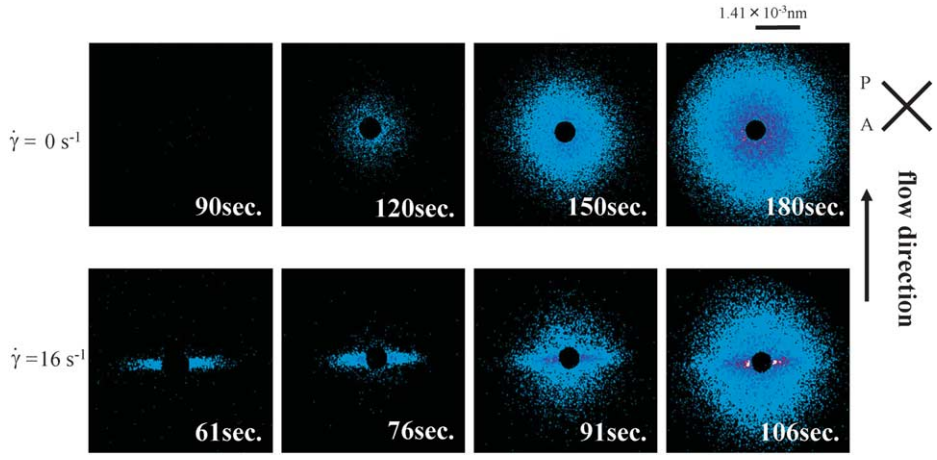

Fig. 2. Time evolution of 2D depolarized light scattering (DPLS) pattern from PE during the crystallization process at 129 °C. Upper: under quiescent condition, lower: after pulse shear with shear rate $\dot{\gamma} = 16\ s^{-1}$ and shear strain $\varepsilon = 3200\%$.

in intensity with annealing time while isotropic component also appears at about 80 s as seen in the lower row in Fig. 2. The isotropic scattering component suggests that some parts of PE are not affected by the shear to produce isotropic structure like spherulite.

We would like to briefly discuss if the shish-like structure is crystal or not (a precursor of the shish) in the early stage during the crystallization process because DPLS measurements can detect any oriented structure whether it is crystal or not. We have performed DSC measurements on the crystallization process of the same PE under the quiescent condition at 129 °C. The result is shown in Fig. 3. After the induction time of about 300 s, exotherm due to the crystallization is observed. On the other hand, DPLS intensity is already observed at 110 s (see Fig. 2). These results imply that the DPLS measurement is so sensitive as to detect a precursor of the shish before the nucleation or a small amount of the (crystallized) shish compared with the DSC measurement. At the moment, it is hard to say which is correct. Hsiao et al. [19] has performed time resolved small-angle X-ray scattering measurements on structural development of isotactic polypropylene (iPP) after applying pulse shear above the nominal melting temperature to find a streak-like scattering normal to the flow direction, corresponding to the shish-like structure. It should be emphasized here that this observation was above the nominal melting temperature, suggesting that the shish-like structure is not crystal. In the present experiment, we did not observe the shish-like structure above the melting temperature, but it is impossible to deny that the observed streak-like scattering pattern is due to the precursor. Hence, we do not use the shish structure, but the shish-like structure here.

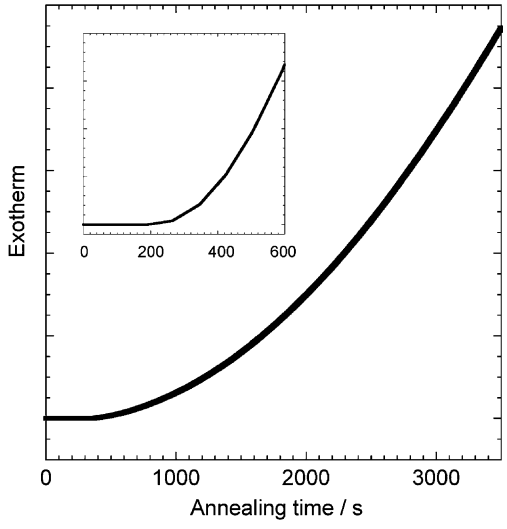

Fig. 3. DSC isotherm of PE at 129 °C after temperature jump from 165 °C. Inset is expansion in the first 600 s after the temperature jump.

We have examined effects of the shear rate $\dot{\gamma}$ and the shear strain ε on the structure formation during the crystallization after pulse shear. Fig. 4 shows time evolutions of 2D DPLS patterns for shear rates $\dot{\gamma}$ of 1, 4 and 16 s^{-1} at a given shear strain ε of 3200%. The scattering patterns are isotropic at both the shear rates of 1 and 4 s^{-1}, while the scattering pattern at $\dot{\gamma} = 4\ s^{-1}$ appears earlier than that at 1 s^{-1}, showing acceleration of the crystallization rate with increasing the shear rate. On the other hand, comparing the scattering patterns between $\dot{\gamma} = 4$ and 16 s^{-1}, the 2D pattern at 16 s^{-1} is anisotropic and shows the streak-like scattering in addition to the acceleration of the crystallization rate. It is clear that the shear rate affects the crystallization rate as well as the anisotropic structure formation. The acceleration is observed at the relatively low shear rates while the anisotropic structure formation is at the relatively high shear rates.

In Fig. 5, the time evolutions of 2D DPLS patterns are shown for various shear strains $\varepsilon = 1600$, 3200 and 6400% at a given shear rate $\dot{\gamma} = 4\ s^{-1}$. Similar to the shear rate effects, the acceleration of the crystallization rate and the appearance of anisotropic scattering patterns are observed as the shear strain increases.

In order to evaluate quantitatively the effects of shear rate

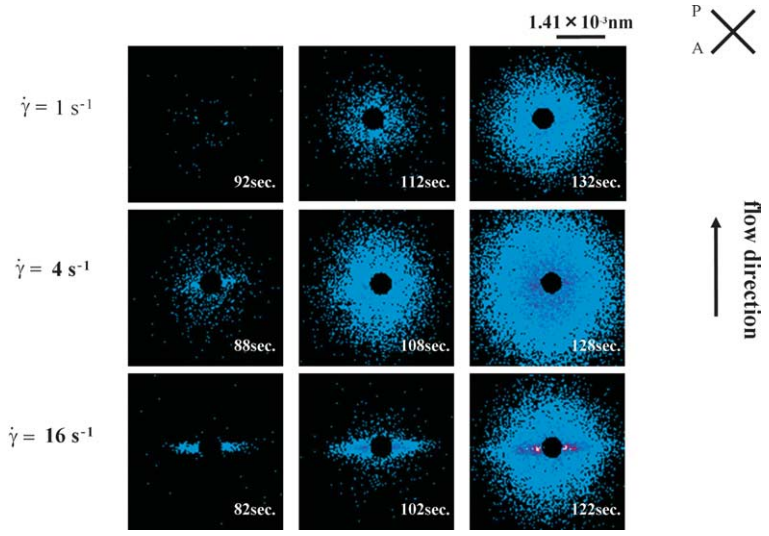

Fig. 4. Time evolution of DPLS pattern form PE during the crystallization process at 129 °C after pulse shear with shear rates $\dot{\gamma} = 1$, 4 and 16 s^{-1} from top to bottom at a given shear strain $\varepsilon = 3200\%$.

on the structure formation, the following two measures are defined in this paper. In Fig. 6 the integrated DPLS intensity normal to the flow direction is plotted as a function of the annealing time for various shear rates $\dot{\gamma}$ at a given shear strain $\varepsilon = 3200\%$. The scattering intensity is very weak in the induction period and abruptly begins to increase. This induction time t_{ind} decreases with increasing the shear rate, showing the acceleration of the crystallization rate. We then employed the induction time t_{ind} as a measure of the acceleration of crystallization rate. Generally speaking, the crystallization rate is dominated by the nucleation rate and the growth rate, and the induction time t_{ind} is mainly governed by the nucleation rate. Therefore, we discuss the acceleration of the nucleation rate due to the shear flow here. The slope of the scattering intensity vs. time after the induction time would be used as a measure of the crystallization rate, especially the growth rate. However, this measure was not employed here because the sample thickness is rather thick so that the scattering intensity is not proportional to the degree of crystallinity in the late stage. Second measure is for the anisotropy. A typical anisotropic 2D scattering pattern is shown in Fig. 7(a) and the corresponding scattering intensities normal and parallel to the flow direction are plotted against Q in Fig. 7(b). In the high Q range the scattering intensities are very weak and begin to increase at certain onset Q values with decreasing Q, depending on the scattering direction. Here we employed a ratio of the onset Q value normal to the flow direction to the parallel one R_{ani} ($= Q_{\perp}/Q_{\parallel}$) as a measure of anisotropy. The onset $Q_{\parallel}$ parallel to the flow direction was sometimes

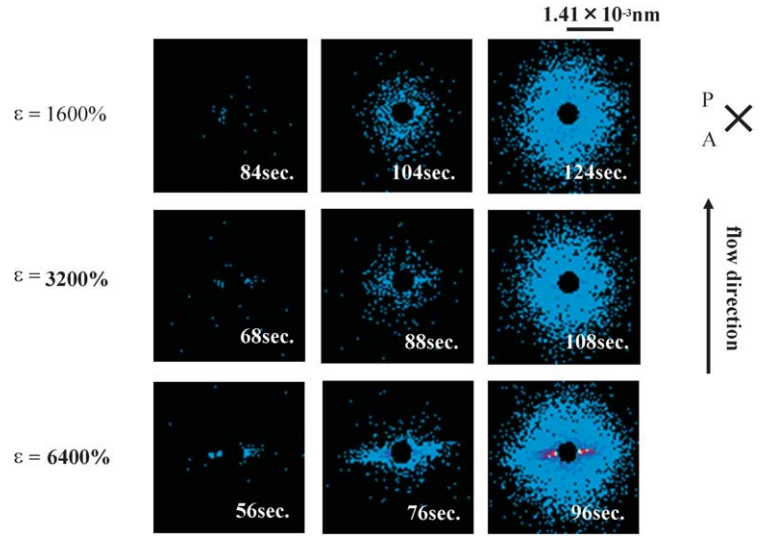

Fig. 5. Time evolution of DPLS pattern form PE during the crystallization process at 129 °C after pulse shear with shear strain $\varepsilon = 1600$, 3200 and 6400% from top to bottom at a given shear rate $\dot{\gamma} = 4$ s^{-1}.

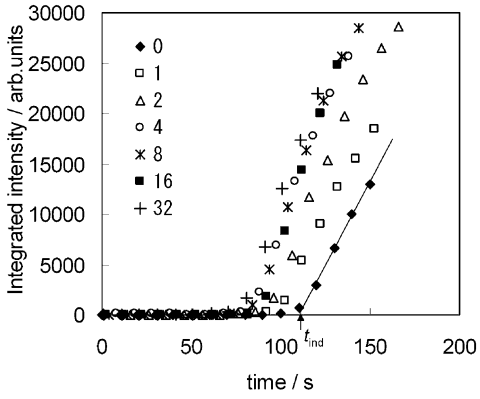

Fig. 6. Time evolution of integrated DPLS intensity of PE at 129 °C normal to the flow direction for various shear rates $\dot{\gamma}$ from 0 to 32 s^{-1}, showing the definition of induction time t_{ind}. The shear strain ε is 3200% for all the measurements.

inside in the beam stopper as shown in Fig. 7(c). In this case we cannot follow the above procedure to determine $Q_{\parallel}$, and hence employed another procedure. We draw the contour curve at a height of d_Q which was used to determine $Q_{\perp}$ (see Fig. 7(d)) and interpolated the contour curve inside the beam stopper. Then, we define the $Q_{\parallel}$ as shown in Fig. 7(c). This definition is slightly different from the first one, but the degree of anisotropy is almost the same within the experimental error. The measure is a sort of aspect ratio of the 2D scattering pattern and called the degree of anisotropy here.

We first examined the shear rate effects on the induction time t_{ind} and the degree of anisotropy R_{ani}. The induction time t_{ind} and the degree of anisotropy R_{ani} are plotted against the logarithm of the shear rate $\dot{\gamma}$ in Fig. 8(a) and (b), where the shear strain ε is kept constant at 3200%. The induction time t_{ind} under the quiescent condition ($\dot{\gamma} = 0$) is about 110 s and decreases with increasing the shear rate. As seen in Fig. 8(a), the linear relationship between the induction time t_{ind} and the logarithm of the shear rate $\dot{\gamma}$ holds, at least in the shear rate range examined although we do not have any theoretical basis for this relation. The relation is given by:

$$\dot{\gamma}_{ind,c} = \dot{\gamma}\exp\left[\frac{t_{ind} - t_{ind,0}}{\tau_{ind}}\right]$$

where $\dot{\gamma}_{ind,c}$, $t_{ind,0}$ and τ_{ind} are the critical shear rate for the induction time, the induction time under quiescent condition and a constant with unit of time. According to the relation, we have extrapolated the induction time to 110 s to find the critical shear rate for the acceleration of the crystallization rate at around $\dot{\gamma}_{ind,c} = 0.4\ s^{-1}$ (Fig. 8(a)). As for the relation between the degree of anisotropy R_{ani} and the logarithm of the shear rate $\dot{\gamma}$, similar linear relation holds experimentally.

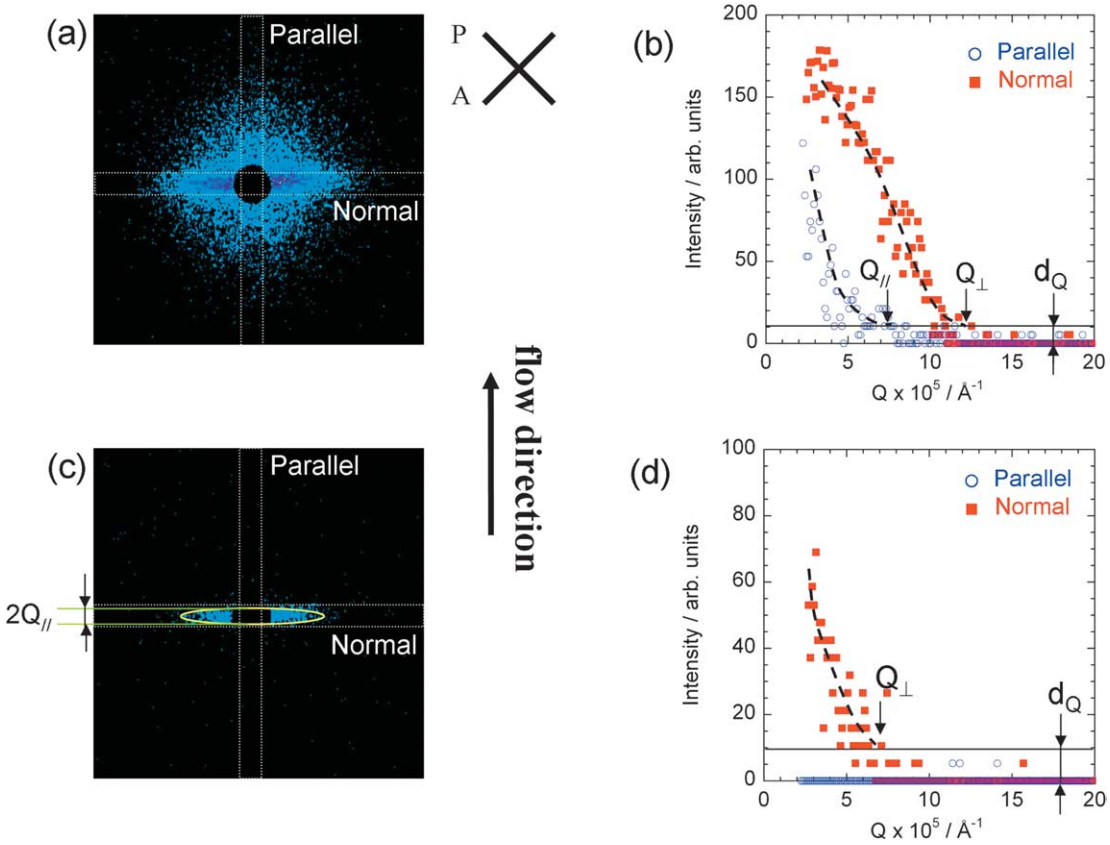

Fig. 7. (a) and (c) Typical 2D DPLS patterns; (b) and (d) the definitions of the degree of anisotropy R_{ani} ($=Q_{\perp}/Q_{\parallel}$) corresponding to (a) and (c), respectively.

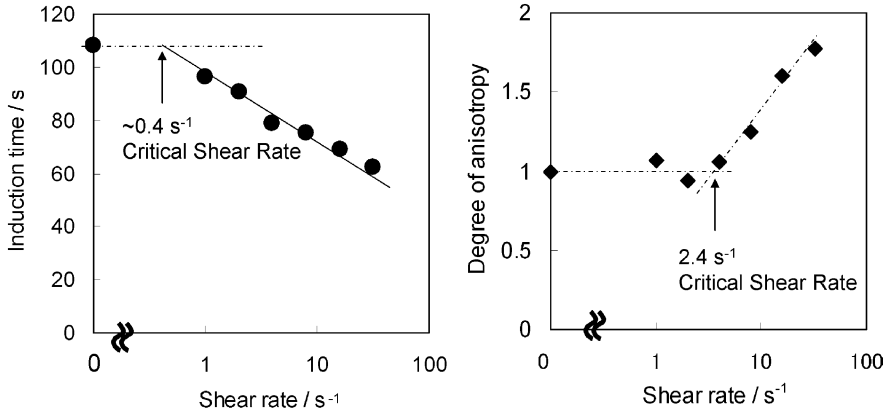

Fig. 8. Shear rate dependence of (a) the induction time t_{ind} and (b) the degree of anisotropy R_{ani}. The shear strain ε is 3200%.

That is given by

$$\dot{\gamma}_{ani,c} = \dot{\gamma}\exp\left[-\frac{R_{ani} - R_{ani,0}}{r_{ani}}\right]$$

where $\dot{\gamma}_{ani,c}$, $R_{ani,0}$ and r_{ani} are the critical shear rate for the anisotropy, the degree of anisotropy under quiescent condition (=1), and a dimensionless constant. We also extrapolated the degree of anisotropy to unity and found the critical shear rate for the anisotropy at around $\dot{\gamma}_{ani,c} = 2.4\ s^{-1}$. This value is much larger than the critical shear rate for the acceleration of crystallization rate $\dot{\gamma}_{ind,c}$ (=0.4 s^{-1}). In other words, the acceleration effect is observed in a low shear rate region while relatively large shear rate is necessary for the anisotropic structure formation. This problem is briefly discussed in terms of chain relaxation in what follows. Applying pulse shear polymer chains are somewhat extended, and after the cessation of the shear they tend to relax to recover the original non-oriented conformations. This process must be governed by the longest relaxation time. On the other hand, the chains want to crystallize because they are in the supercooled state below the melting temperature although the crystallization rate is not fast at the present T_c (=129 °C) under quiescent condition, meaning that there must be a competition between the crystallization and the relaxation. In the present DPLS experiments, we observed that the detector screen was completely dark at 2 or 3 s after the cessation of the shear, suggesting the polymer chains completely relax to the original non-oriented conformation, at least in a length scale of light scattering. However, we observed the acceleration of the crystallization rate or the reduction in the induction time. This may mean that the local orientation remains in the chains, which induces the crystallization (orientation-induced crystallization). At the shear rates below the critical value for the anisotropy $\dot{\gamma}_{ani,c}$, the orientation must be too local to result in the anisotropic structure (the shish-like structure) in the light scattering scale. As the shear rate increases above the critical value $\dot{\gamma}_{ani,c}$, the chains are more extended and crystallize earlier before the relaxation in the extended conformation, resulting in the anisotropic structure in the light scattering scale.

In the next we have determined the critical shear rates as a function of shear stain. The critical shear rate for the induction time $\dot{\gamma}_{ind,c}$ was almost zero at the shear strains above 3200%, and hence it was hard to estimate the shear strain dependence of the critical shear rate $\dot{\gamma}_{ind,c}$ in the experimental accuracy. Therefore, we focus on the shear strain dependence of the critical shear rate for the degree of anisotropy $\dot{\gamma}_{ani,c}$. In Fig. 9, the degree of anisotropy R_{ani} is plotted against the logarithm of the shear rate $\dot{\gamma}$ for various shear strains, where the data in Fig. 8(b) is also included. As seen in figure, the critical shear rate for the degree of anisotropy $\dot{\gamma}_{ani,c}$ decreases with increasing the shear strain. The linear relation between the degree of anisotropy R_{ani} and the logarithm of the shear rate $\dot{\gamma}$ holds for all the shear strains examined in this study. Extrapolating the degree of anisotropy to unity we have evaluated the critical shear rate as a function of the shear strain, and plotted against the inverse of the shear strain in Fig. 10. The plot shows a good

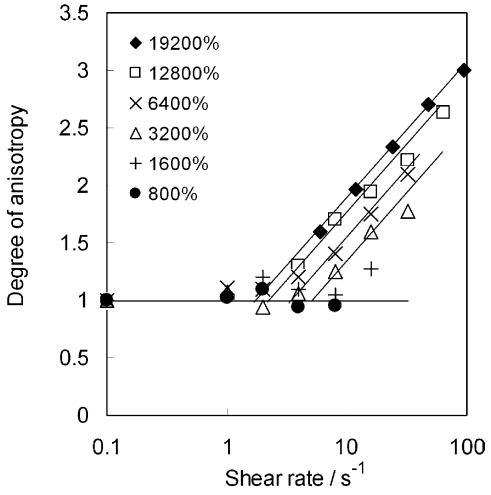

Fig. 9. Shear rate dependence of the degree of anisotropy R_{ani} for various shear strains ε from 800% to 19,200%.

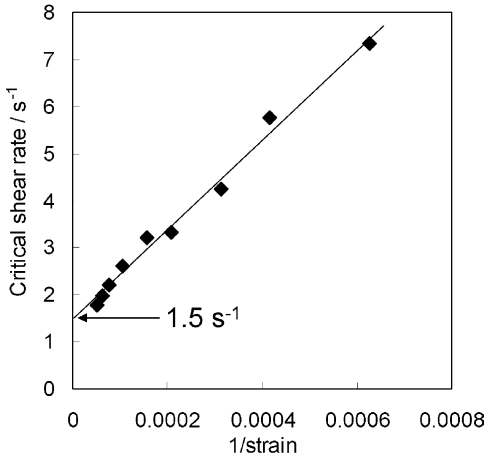

Fig. 10. Critical shear rate for the anisotropy $\dot{\gamma}_{ani,c}$ against inverse of shear strain ε.

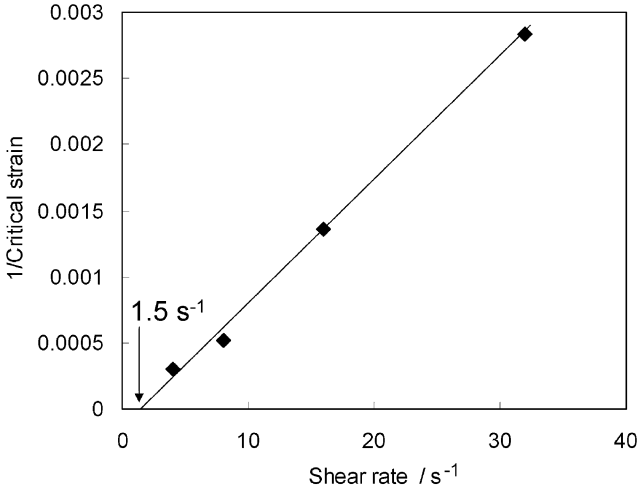

Fig. 12. Inverse of critical shear strain $1/\varepsilon_{ani,c}$ against shear rate $\dot{\gamma}$.

linear relationship. Extrapolating this linear relationship to the inverse of the shear strain = 0, we found that the critical shear rate at the infinite shear strain is about 1.5 s^{-1}. This corresponds to the critical shear rate under continuous shear flow.

The same analysis has been done on the shear strain dependence of the degree of anisotropy R_{ani}. The degree of anisotropy R_{ani} is plotted against the shear strain for various shear rates of 1–32 s^{-1} in Fig. 11. In this plot, we also assumed that the linear relationship holds between the degree of anisotropy R_{ani} and the logarithm of shear strain ε. Note that the anisotropy at the low shear rates below 4 s^{-1} is very low and not reliable. Extrapolating the linear relation to the degree of anisotropy = 1, we have evaluated the critical shear strain at each shear rate, and the inverse of the critical shear stain is plotted against the shear rate in Fig. 12, giving a straight line. Again, extrapolating this relation to inverse of the critical shear strain = 0, we have evaluated the critical shear rate at the infinite shear strain to be 1.5 s^{-1}. This value agrees very well with the critical shear rate at the infinite shear strain evaluated from the relation between the

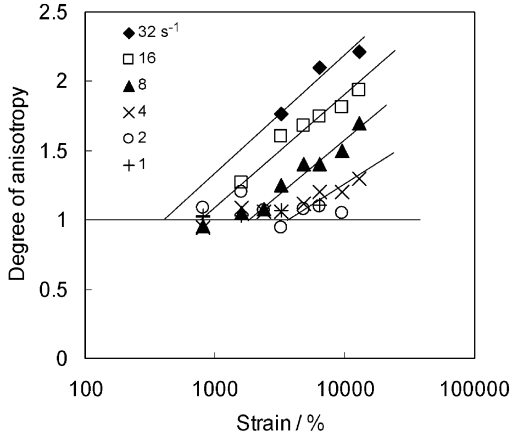

Fig. 11. Shear strain dependence of the degree of anisotropy R_{ani} for various shear rates $\dot{\gamma}$ from 1 to 32 s^{-1}.

critical shear rate and the inverse of shear strain (see Fig. 10). This suggests the validity of the analysis. Here we would like to consider a possible physical meaning of the critical shear rate at the infinite shear strain, which must correspond to the continuous shear flow. In this situation, the extension of polymer chain is almost dominated by the relation between the shear rate $\dot{\gamma}$ and the longest relaxation time τ. If the shear rate is larger than the relaxation rate (or inverse of the relaxation time) τ^{-1}, the polymer chains are somewhat extended and oriented under the flow. The polymer chains are in the supercooled state below the melting temperature, and hence tend to crystallize. The orientation must accelerate the crystallization rate (orientation-induced crystallization). Thus, the critical shear rate is related to the relaxation rate: $\dot{\gamma}_{ani,c} \sim \tau^{-1}$, if we neglect a numerical factor in order of unity. This is one of tentative scenarios for the shish formation in the early stage of crystallization. In order to confirm this scenario it must be essential to examine effects of the molecular weight distribution and the rheological properties on the crystallization.

4. Conclusion

Here we have investigated the structure formation of PE in the early stage during the crystallization after pulse shear using depolarized light scattering (DPLS), focusing on the effects of the shear rate and the shear strain. The objective of this study is to elucidate the formation mechanism of the so-called shish-kebab structure. In the early stage during the crystallization after pulsed shear 2D DPLS pattern clearly shows the streak-like scattering normal to the flow direction, suggesting the formation of shish-like structure in μm scale along the flow. Defining measures for the acceleration of the crystallization rate and the degree of anisotropy, we have determined the critical shear rate for both of the measures at a given shear strain, and found that the critical shear rate for

the former is much smaller than the latter. Analyzing the shear strain dependence of the critical shear rate for the anisotropy we have estimated the critical shear rate at the infinite shear strain, which must correspond to the continuous flow. This critical shear rate was discussed in relation to the competition between the chain relaxation and the orientation-induced crystallization rate.

References

[1] Ward IM. Structure and properties of oriented polymers. New York: Wiley; 1975.
[2] Ziabicki A. Fundamentals of fiber formation. New York: Wiley; 1976.
[3] Keller A, Kolnaar JWH. In: Meijer HEH, editor. Processing of polymers. New York: VCH; 1997. p. 189–268.
[4] Walczak ZK. Processses of fiber formation. Elsevier: Amsterdam; 2002.
[5] Pennings AJ, Kiel AM. Colloid Z Z Polym 1965;205:160–2.
[6] Pennings AJ. J Polym Sci: Part C: Polym Symp 1977;59:55–86.
[7] Odell JA, Grubb DT, Keller A. Polymer 1978;19:617–26.
[8] Bashir Z, Odell JA, Keller A. J Mater Sci 1984;19:3713–25.
[9] Bashir Z, Odell JA, Keller A. J Mater Sci 1986;21:3993–4002.
[10] Samon JM, schultz JM, Hsiao BS, Seifert S, Stribeck N, Gurke I, Collins G, Saw C. Macromolecules 1999;32:8121–32.
[11] Samon JM, Schultz JM, Wu J, Hisao BS, Yeh F, Kolb R. J Polym Sci: Part B: Polym Phys 1999;37:1277–87.
[12] Somani RH, Hsiao BS, Nogales A, Srinivas S, Tsuo AH, Sics I, et al. Macromolecules 2000;33:9385–94.
[13] Schultz JM, Hsiao BS, Samon JM. Polymer 2000;41:8887–95.
[14] Samon JM, Schultz JM, Hisao BS, Wu J, Khot S. J Polym Sci: Part B: Polym Phys 2000;38:1872–82.
[15] Samon JM, Schultz JM, Hsiao BS, Khot S, Johnson HR. Polymer 2001;42:1547–59.
[16] Nogales A, Somani RH, Hsiao BS, Srinivas S, Tsuo AH, Balta-Calleja J, et al. Polymer 2001;42:5247–56.
[17] Somani RH, Hsiao BS, Nogales A, Fruitwala H, Srinivas S, Tsuo AH. Macromolecules 2001;34:5902–9.
[18] Somani RH, Young L, Hsiao BH, Agarwal PK, Fruitwala HA, Tsuo AH. Macromolecules 2002;35:9096–104.
[19] Somani RH, Yang L, Hsiao BS. Physica A 2002;304:145–57.
[20] Yang L, Somani RH, Sics I, Hsiao BH, Kolb R, Fruitwala H, et al. Macromolecules 2004;37:4845–59.
[21] Pogodina NV, Siddiquee SK, Egmond JWv, Winter HH. Macromolecules 1999;32:1167–74.
[22] Pogodina NV, Lavrenko VP, Srinivas S, Winter HH. Polymer 2001; 42:9031–43.
[23] Elmoumni A, Winter HH, Waddon AJ, Fruitwala H. Macromolecules 2003;36:6453–61.
[24] Kumaraswamy G, Issaian AM, Kornfield JA. Macromolecules 1999; 32:7537–47.
[25] Kumaraswamy G, Verma RK, Issaian AM, Wang P, Kornfield JA, Yeh F, et al. Polymer 2000;41:8934–40.
[26] Kumaraswamy G, Kornfield JA, Yeh F, Hsiao B. Macromolecules 2002;35:1762–9.
[27] Kolb K, Seifert S, Stribeck N, Zachmann HG. Polymer 2000;41: 2931–5.
[28] Kolb R, Seifert S, Stribeck N, Zachmann HG. Polymer 2000;41: 1497–505.
[29] Jerschow P, Janeschitz-Kriegel H. Int Polym Process 1997;12:72–7.
[30] Nogami K, Murakami S, Katayama K, Kobayashi K. Bull Inst Chem Res. Kyoto Univ 1977;55:227–36.